J Mol Model (2013) 19:3219–3224
DOI 10.1007/s00894-013-1846-4

ORIGINAL PAPER

$[(B_3O_3H_3)_nM]^+$(n=1, 2;M=Cu, Ag, Au): a new class of metal-cation complexes

Da-Zhi Li · Chen-Chu Dong · Shi-Guo Zhang

Received: 31 January 2013 / Accepted: 2 April 2013 / Published online: 1 May 2013

Abstract A density functional theory (DFT) investigation into the structures and bonding characteristics of $[(B_3O_3H_3)_nM]^+$(n=1, 2;M=Cu, Ag, Au) complexes was performed. DFT calculations and natural bond orbital (NBO) analyses indicate that the IB metal complexes of boroxine exhibit intriguing bonding characteristics, different from the typical cation–π interactions between IB metal-cations and benzene. The complexes of $[B_3O_3H_3M]^+$ and $[(B_3O_3H_3)_2M]^+$ (M=Cu, Ag, and Au) favor the conformation of perfectly planar structures with the C_{2v} and D_{2h} symmetry along one of the threefold molecular axes of boroxine, respectively. Detailed natural resonance theory (NRT) and canonical molecular orbitals (CMOs) analyses show that interaction between the metal cation and the boroxine in $[B_3O_3H_3M]^+$ (M=Cu, Ag, and Au) is mainly ionic, while the IB metal-cations←π donation effect is responsible for the binding site. In these complexes, boroxine serves as terminals η^1-$B_3O_3H_3$ with one O atom of the B_3O_3 ring. The infra-red (IR) spectra of $[B_3O_3H_3M]^+$ were simulated to facilitate their future experimental characterization. The complexes all give two IR active modes at about 1,300 and 2,700 cm^{-1}, which are inactive in pure boroxine. Simultaneously, the B–H stretching modes of the complexes are red-shifted due to the interaction between the metal-cation and boroxine. To explore the possibility of the structural pattern developed in this work forming mesoporous materials, complexes $[(B_3O_3H_3M)_6]^{6+}$ (M=Cu, Ag, and Au) were also studied, which appear to be unique and particular interesting: they are all true minima with D_{6h} symmetries and pore sizes ranging from 12.04 Å to 13.65 Å.

Keywords Boroxine · Metal-cation complex · Density functional theory · Geometric structure · Bonding characteristic

Introduction

As an inorganic analogue of benzene, boroxine $B_3O_3H_3$ shares many similarities with benzene both in structures and characteristics. Series of studies on its preparation, geometrical structures, and electronic characteristics has been performed [1–7]. In 2005, boroxines were thrust into the spotlight when the Yaghi group [8] published a landmark paper describing the synthesis and characterization of the first crystalline arylboroxine-based covalent organic framework (COF-1) material. Since the disclosure of COF-1, B_3O_3 ring systems have been studied widely as organizing elements, molecules of fundamental interest, and linkages in solid-state materials [9–12]. Benzene is a good prototype aromatic compound and serves as a model for π systems. Recent studies have revealed that metal-ion–benzene complexes are of particular interest for their relevance to catalytic and biological processes [13, 14]. A series of metal-ion–benzene complexes, including half-sandwich complexes with the cations (Na^+, Cu^+, and Ag^+) above the benzene centroid [15–21], full-sandwich complexes, M^+Bz_2 (M=Sc–Cu) with the metal atom enclosed by two parallel benzene rings with staggered D_{6d} or eclipsed D_{6h} high-symmetry [22], and multidecker sandwich molecular wires with D_{3h} $B_3N_3H_6$ or D_{6h} C_6H_6 as ligands [23, 24], have been studied widely. However, to the best of our knowledge,

Electronic supplementary material The online version of this article (doi:10.1007/s00894-013-1846-4) contains supplementary material, which is available to authorized users.

D.-Z. Li (✉) · C.-C. Dong · S.-G. Zhang
Binzhou Key Laboratory of Material Chemistry, Department of Chemistry and Chemical Engineering, Binzhou University, Binzhou 256603, People's Republic of China
e-mail: ldz005@126.com

no metal-cation complexes with $B_3O_3H_3$ as ligands have been reported to date in the literature. In this work, we present an investigation of a new class of metal-cation boroxine complexes of ion–benzene (IB). Detailed natural resonance theory (NRT), canonical molecular orbitals (CMOs) and IR spectra analyses are used to explore the interaction between the IB metal cation and the boroxine in $[B_3O_3H_3M]^+$ and $[(B_3O_3H_3)_2\ M]^+$ (M=Cu, Ag, and Au).

Computational methods

Density functional theory (DFT) structural optimization was performed on the planar, half-sandwich, and sandwich complexes under investigation and imaginary frequencies using the B3LYP [25, 26] and PBE1PBE [27] methods, respectively. Relative energies for the different types of complexes were further refined using the coupled cluster method with triple excitations [CCSD(T)] [28–30] at B3LYP geometries. NRT was used to calculate bond orders and bond polarities. The Stuttgart relativistic small core basis set and effective core potential (Stuttgart RSC 1997 ECP) [31] was employed for Cu, Ag, and Au, and the 6−311+G(d,p) basis implemented in Gaussian03 program [32] for B, H, and O. The NBO5.0 [33] program was used to calculate bond orders and atomic charges. Figure 1 shows the optimized planar structures of $[B_3O_3H_3M]^+$ at the B3LYP level. For comparison, the optimized M^+Bz complexes at the same level are also listed in Fig. 1. The optimized planar structures of $[(B_3O_3H_3)_2M]^+$ (M=Cu, Ag, and Au) at B3LYP are given in Fig. 2. Figure 3 shows some typical occupied MOs involving M 3d and the delocalized π orbitals of C_{2v} $[B_3O_3H_3M]^+$ (M=Cu, Ag, and Au). Figure 4 depicts the simulated IR spectra of the planar C_{2v} $[B_3O_3H_3M]^+$. The optimized structures of the $[(B_3O_3H_3M)_6]^{6+}$ (M=Cu, Ag, Au) at B3LYP level are shown in Fig. 5. Table 1 tabulates the NRT bond orders, covalent (CNRT) and ionic (INRT) of metal-O for planar $[B_3O_3H_3M]^+$ and $[(B_3O_3H_3)_2]M^+$ (M=Cu, Ag, and Au) with C_{2v} symmetry. The lowest vibrational frequencies (ν_{min}) and intermolecular mode frequencies (ν_i) of the complexes at B3LYP and PBE1PBE level are tabulated in Table 2.

Results and discussion

C_{2v} $[B_3O_3H_3\ M]^+$

We start from $[B_3O_3H_3M]^+$, the simplest complex studied in this work. As clearly shown in Fig. 1 and Fig. S1, C_{2v} $[B_3O_3H_3Cu]^+$ ($^1A_1$) **1** possesses a perfectly planar structure with an O–Cu bond length of 1.94 Å, which lies 1.21 and 1.11 eV lower than the half-sandwich structure at B3LYP and B3LYP//CCSD(T), respectively. The C_{2v} $[B_3O_3H_3Cu]^+$ **1** is different from that of Cu^+Bz [22], which is believed to possess a half-sandwich structure (C_{6v}) with the metal cation lying on top of the benzene ring. Differing from those of Ag^+Bz and Au^+Bz, the lowest-lying planar structures of C_{2v} $[B_3O_3H_3Ag]^+$ **2** and C_{2v} $[B_3O_3H_3Au]^+$ **3** can also be obtained by attaching a terminal Ag or Au atom to one O atom of the B_3O_3 ring along one of the threefold molecular axes (see Fig. 1), i.e., Cu^+, Ag^+ and Au^+ cations favor the π_{off} structure when they interact with boroxine. We also note that the D_{3h} $B_3O_3H_3$ is well maintained in C_{2v} $[B_3O_3H_3M]^+$ complexes. PBE1PBE computations with corresponding basis sets confirmed that C_{2v} $[B_3O_3H_3Cu]^+$ **1**, C_{2v} $[B_3O_3H_3Ag]^+$ **2** and C_{2v} $[B_3O_3H_3Au]^+$ **3** are all true minima with no imaginary frequencies (see Table 2). It should be noted that the half-sandwich form of $[B_3O_3H_3Cu]^+$, $[B_3O_3H_3Ag]^+$, and $[B_3O_3H_3Au]^+$ are all transition states, each with two imaginary frequencies over 80 cm^{-1} at B3LYP level.

D_{2h} $[(B_3O_3H_3)_2\ M]^+$

The second series of complexes of IB metal-cations interacting with boroxine in this work is $[(B_3O_3H_3)_2\ M]^+$

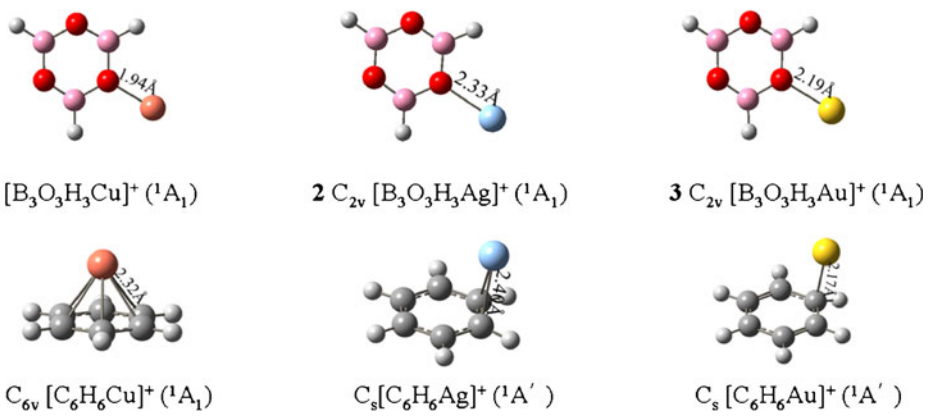

Fig. 1 Optimized structures of the $[B_3O_3H_3M]^+$ (M=Cu, Ag, Au) at B3LYP level

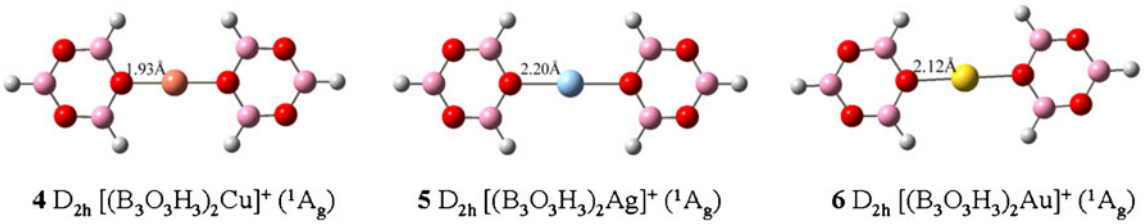

Fig. 2 Optimized structures of the $[(B_3O_3H_3)_2\ M]^+$ (M=Cu, Ag, Au) at B3LYP level

(M=Cu, Ag, and Au). As shown in Fig. 2 and Fig. S2, the planar D_{2h} $[(B_3O_3H_3)_2Cu]^+$ **4**, with a bond length of $r_{O–Cu}$= 1.93 Å lies 2.47 and 2.30 eV lower than the sandwich-type structure at B3LYP and B3LYP//CCSD(T), respectively. Similar to $[B_3O_3H_3Cu]^+$ **1** with C_{2v} symmetry, the D_{2h} $[(B_3O_3H_3)_2Cu]^+$ is different from that of sandwich complexes Cu^+Bz_2 [21, 22], with the metal atom being enclosed by two parallel benzene rings with suggested high-symmetry confirmations that are either staggered D_{6d} or eclipsed D_{6h}. For $[(B_3O_3H_3)_2Ag]^+$ and $[(B_3O_3H_3)_2Au]^+$, the perfectly planar structure **5** and **6** with $r_{O–Ag}$=2.20 Å and $r_{O–Au}$=2.21 Å are low-lying structures, respectively (Fig. 2). Just as the situation in C_{2v} $[B_3O_3H_3M]^+$ series, the D_{3h} $B_3O_3H_3$ is well maintained in D_{2h} $[(B_3O_3H_3)M]^+$ complexes. PBE1PBE computations with corresponding basis sets confirmed the B3LYP structures and vibrational frequency analyses. The sandwich forms of $[(B_3O_3H_3)_2Cu]^+$, $[(B_3O_3H_3)_2Ag]^+$, and $[(B_3O_3H_3)_2Au]^+$ are all also transition states with five imaginary frequencies (among them four are over 100 cm^{-1} at B3LYP level), respectively. We also note that, as conformational isomers, the D_{2d} $[(B_3O_3H_3)M]^+$ (M=Cu, Ag, and Au) listed in Fig. S2 lie very close in energy at the B3LYP and CCSD(T)//B3LYP level and may coexist in experiments. The $D_{2h}\rightarrow D_{2d}$ rotatory transition for $[(B_3O_3H_3)_2Cu]^+$, $[(B_3O_3H_3)_2Ag]^+$, and $[(B_3O_3H_3)_2Au]^+$ has energy barriers of only −0.06, 0.02 and 0.18 kcal/mol at CCSD(T)//B3LYP levels, respectively.

Bonding characteristics

Natural bond orbital (NBO) analyses were carried out to gain a deeper understanding of the bonding characteristics in these systems. The atomic charges were calculated using B3LYP calculations based on NBO population analysis. As expected and confirmed, the positive charges of the C_{2v} $[B_3O_3H_3M]^+$ cations are concentrated mainly on the metal atoms, which carry the high net atomic charge of q_{Cu}=+ 0.92, q_{Ag}=+0.94, and q_{Au}=+0.86, respectively, i.e., the charge transfer from Cu^+, Ag^+ or Au^+ to boroxine is insignificant. This may be associated with the d^{10} electron configuration of Cu^+, Ag^+ and Au^+.

The detailed NRT-calculated results further confirm the weak charge transfer. As shown in Table 1, the O-metal interactions in C_{2v} $[B_3O_3H_3M]^+$ are mainly ionic. For Cu–O, Ag–O, and Au–O, the calculated NRT bonds and INRT bonds are 0.043 and 0.040, 0.033 and 0.031, and 0.075 and 0.086, respectively. Clearly, the electrovalent bonds are primary although the interactions are weak. So, like that of metal cation benzene complexes [21, 22], the bonding in metal-cation boroxine complexes is primarily electrostatic. The electrostatic interaction contribution to the benzene complexes with an alkali metal-cation decreases as the distance between the metal cation and the benzene centroid increases [34–36]. However, such a trend is not observed for the boroxine complexes with Cu^+, Ag^+ and Au^+ due to the strong relativistic effects of Au.

Detailed canonical molecular orbitals (CMOs) analyses can help to understand the bonding patterns between the metal cation and boroxine. Here, we discuss the case of planar C_{2v} $[B_3O_3H_3M]^+$. As clearly shown in Fig. 3, the typical occupied MOs can be unambiguously assigned to the interactions of delocalized π orbitals of D_{3h} $B_3O_3H_3$ ligand and the 3d orbitals of Cu^+, Ag^+, and Au^+ center. For C_{2v} $[B_3O_3H_3Cu]^+$, HOMO-8(b_1) and HOMO-12(b_1) reflect the interactions between the delocalized π MOs of

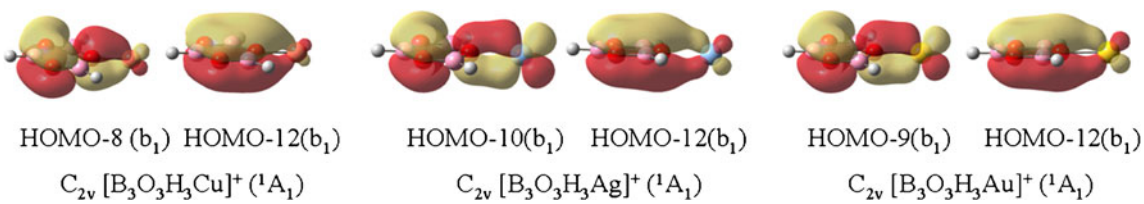

Fig. 3 Some typical occupied molecular orbitals (MOs) involving M 3d and the delocalized π orbitals of C_{2v} $[B_3O_3H_3M]^+$ (M=Cu, Ag, Au) structures at B3LYP level

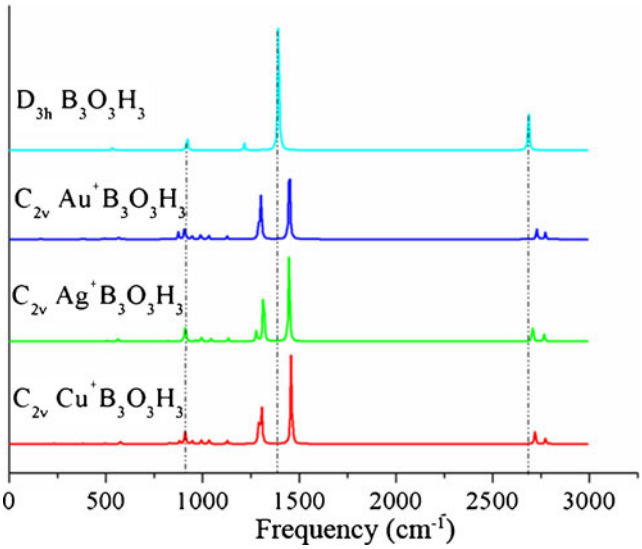

Fig. 4 Simulated infra red (IR) spectra of optimized C_{2v} $M^{+}B_3O_3H_3$ (M=Cu, Ag, Au)

the $B_3O_3H_3$ with the $3d_{xy}$ and $3d_{x2-y2}$ orbitals of the Cu^{+} center. We also note that the typical MOs of C_{2v} $[B_3O_3H_3Ag]^{+}$ and $[B_3O_3H_3Au]^{+}$ are similar to that of C_{2v} $[B_3O_3H_3Cu]^{+}$. Clearly, in contrast to the electrovalent bonds in alkali metal-cation complexes [34–36], the O-Metal interactions in C_{2v} $[B_3O_3H_3M]^{+}$ are mainly ionic, while the IB metal-cations←π donation effect exists and may be responsible for the binding site.

The binding of Cu^{+}, Ag^{+} or Au^{+} with boroxine brings about IR spectral changes of the boroxine moiety. Figure 4 shows the simulated IR spectra of C_{2v} $M^{+}B_3O_3H_3$ (M=Cu, Ag, Au) as compared to pure boroxine at B3LYP level. The complexes all give two IR active modes at about 1,300 and 2,700 cm^{-1} corresponding to B–H in plane bending mode and the B–H asymmetry stretching vibration, respectively, which are inactive in the pure boroxine. Simultaneously, the ring distortion and B–H stretching modes are red-shifted, due partly to the polarization of the B–H bond reduced by the interaction between Cu^{+}, Ag^{+} or Au^{+} and boroxine.

D_{6h} *[(M $B_3O_3H_3$)$_6$]$^{6+}$*

Now that we know that boroxine serve as terminals η^1-$B_3O_3H_3$ with one O atom of the B_3O_3 ring when boroxine interacts with IB metal-cations, can boroxine be used as a unit, like a B_3O_3 ring, to form mesoporous materials? Figure 5 shows the optimized structures of $[(B_3O_3H_3M)_6]^{6+}$ (M=Cu, Ag, Au) at B3LYP level. Table 2 lists the lowest vibrational frequencies (ν_{min}) and intermolecular mode frequencies (ν_i) in cm^{-1} of the complexes at B3LYP and BPE1BPE level, respectively. Clearly, they appear to be unique and are particular interesting in that they are all true minima with D_{6h} symmetries and pore sizes ranging from 12.04 Å to 13.65 Å at B3LYP level. Interestingly, the structures of $[(B_3O_3H_3M)_6]^{6+}$ (M=Cu, Ag, Au) (presented in Fig. 5) can be derived from that of COF-1 [8] by replacing each benzene ring with a Cu^{+}, Ag^{+}, or Au^{+} cation and each B–C bond with a O-Cu^{+}, O-Ag^{+}, or O-Au^{+} unit. COF-1[8] has been designed and synthesized successfully by a condensation reaction of diboronic acid. Mesoporous materials including D_{6h} $(B_3O_3H_3Cu)_6]^{6+}$, $(B_3O_3H_3Ag)_6]^{6+}$, or $(B_3O_3H_3Au)_6]^{6+}$ may be synthesized in the near future.

Conclusions

The typical half-sandwich structure (C_{6v}) with the metal cation lying on top of the benzene ring and full-sandwich structure either staggered D_{6d} or eclipsed D_{6h} with the metal atom being enclosed by two parallel benzene rings has been studied extensively [18–22, 34–36]. Here, we predicted a

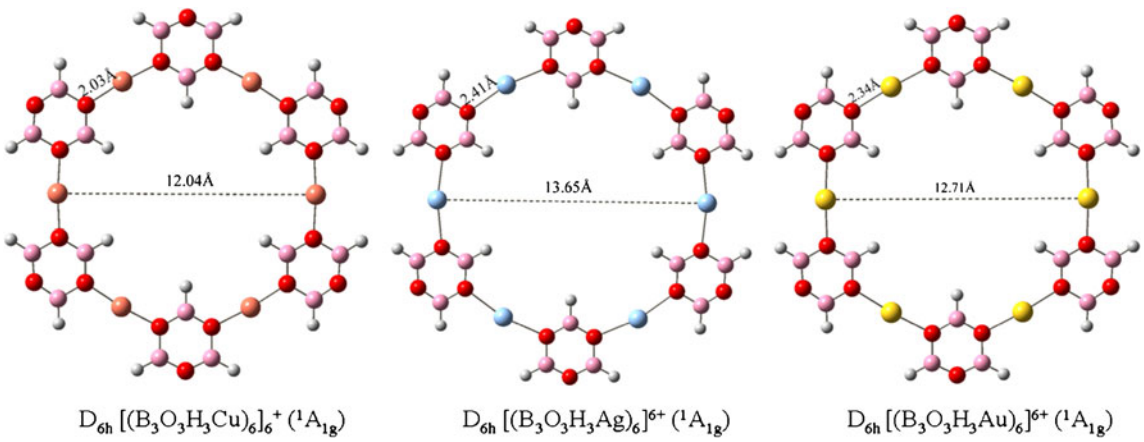

Fig. 5 Optimized structures of $[(B_3O_3H_3M)_6]^{6+}$ (M=Cu, Ag, Au) at B3LYP level

Table 1 Calculated natural resonance theory (NRT) bond orders, covalent (CNRT) and ionic (INRT) of metal-O in C_{2v} $Cu^+B_3O_3H_3(^1A_1)$, C_{2v} $Ag^+B_3O_3H_3(^1A_1)$ and C_{2v} $Au^+B_3O_3H_3(^1A_1)$ at B3LYP level

	NRT	CNRT	INRT
Cu-O	0.043	0.003	0.04
Ag-O	0.033	0.002	0.031
Au-O	0.075	0.007	0.068

new class of metal-cation-boroxine complexes with perfectly planar structures using B3LYP and PBE1PBE methods. Detailed NRT, NBO, and CMOs analyses show that the interaction between the metal cation and the boroxine in the lowest-lying structures of $[B_3O_3H_3M]^+$ (M=Cu, Ag, and Au) are weak electronic interactions, in which boroxine serves only as terminals η^1-$B_3O_3H_3$ with one O atom of the B_3O_3 ring, and the metal-cations←π donation effect being responsible for the binding site. The planar C_{2v} $[B_3O_3H_3M]^+$ (M=Cu, Ag, and Au) complexes show two IR active frequencies at about 1,300 and 2,700 cm^{-1}, corresponding to the B–H in plane-bending mode and the asymmetry stretching vibration, respectively, which are inactive in pure boroxine. Recently, series studies on D_{3h} $B_3N_3H_6$ and D_{6h} C_6H_6 being used as ligands to form multidecker sandwiches on molecular wires has been reported [18, 37–40] due to the intriguing electronic and magnetic properties of multidecker linear organometallic sandwich clusters and their infinite 1D molecular wires. The planar structural pattern developed in this work may be extended to form mesoporous materials. Through their molecular building blocks mesoporous materials may provide ionic frameworks that could be functionalized for gas storage and catalytic applications.

Table 2 Lowest vibrational frequencies (ν_{min}) and intermolecular mode frequencies (ν_i) in cm^{-1} of the complexes at B3LYP and BPE1BPE level

Isomers	ν_{min}		ν_i	
	B3LYP	BPE1BPE	B3LYP	BPE1BPE
C_{2v} $[B_3O_3H_3Cu]^+$	89.13	87.51	232.12	229.91
C_{2v} $[B_3O_3H_3Ag]^+$	87.28	80.72	169.94	169.73
C_{2v} $[B_3O_3H_3Au]^+$	81.45	78.51	165.87	167.28
D_{2h} $[(B_3O_3H_3)_2Cu]^+$	14.64	12.51	155.47	154.09
D_{2h} $[(B_3O_3H_3)_2Ag]^+$	11.47	9.99	125.4	124.71
D_{2h} $[(B_3O_3H_3)_2Au]^+$	18.06	15.94	151.37	155.02
D_{6h} $[(B_3O_3H_3Cu)_6]^{6+}$	11.72	11.42	138.67	134.29
D_{6h} $[(B_3O_3H_3Ag)_6]^{6+}$	7.04	10.80	83.82	76.05
D_{6h} $[(B_3O_3H_3Au)_6]^{6+}$	3.14	4.42	125.15	128.99

Acknowledgments This research was supported by the Research Fund of Binzhou University, China. (2012Y02).

References

1. Barton L, Grimm FA, Porter RF (1966) Inorg Chem 5:2076–2078
2. Chakg CH, Porter RF, Baler SH (1969) Inorg Chem 8:1689–1693
3. Tossell JA, Lazzeretti P (1990) J Phys Chem 94:1723–1724
4. Krishna LB, George DM, Joseph DL, Charles WB (2011) J Phys Chem A 115:7785–7793
5. Grimm FA, Barton L, Forter RF (1968) Inorg Chem 7:1309–1316
6. Gupta SK, Porter RF (1964) J Phys Chem 68:1443–1447
7. Fowler PW, Steiner E (1997) J Phys Chem A 101:1409–1413
8. Côté AP, Benin AI, Ockwig NW, Matzger AJ, O'Keeffe M, Yaghi OM (2005) Science 310:1166–1170
9. Cao D, Wang JL, Smit B (2009) Angew Chem Int Ed 48:4730–4733
10. El-Kaderi HM, Hunt JR, Mendoza-Cortes JL, Cote AP, Taylor RE, O'Keeffe M, Yaghi OM (2007) Science 316:268–272
11. Han SS, Furukawa H, Yaghi OM, Goddard WA (2008) J Am Chem Soc 130:11580–11581
12. Maly KE (2009) J Mater Chem 19:1781–1787
13. Ma JC, Dougherty DA (1997) Chem Rev 97:1303–1324
14. Caldwell JW, Kollman PA (1995) J Am Chem Soc 117:4177–4178
15. Dunbar RC (2000) J Phys Chem A 104:8067–8074
16. Gapeev A, Dunbar RC (2001) J Am Chem Soc 123:8360–8365
17. Ruan CH, Rodgers MT (2004) J Am Chem Soc 126:14600–14610
18. Wang JL, Acioli PH, Jellinek J (2005) J Am Chem 127:2812–2813
19. Alexandrova AN, Boldyrev AI, Fu YJ, Wang XB, Wang LS (2004) J Chem Phys 121:5709–5719
20. Alexandrova AN, Boldyrev AI (2005) J Chem Theory Comput 1:566–580
21. Yi HB, Lee HM, Kim KS (2009) J Chem Theory Comput 5:1709–1717
22. Wedderburn KM, Bililign S, Levy M, Gdanitz RJ (2006) J Chem Phys 326:600–604
23. Hoshino K, Kurikava T, Takeda H, Nakajima A, Kaya K (1995) J Phys Chem 99:3053–3055
24. Li Y, Baer T (2002) J Phys Chem A 106:9820–9826
25. Becke AD (1993) J Chem Phys 98:5648–5652
26. Lee C, Yang W, Parr RG (1988) J Phys Rev B 37:785–789
27. Perdew JP, Burke K, Ernzerhof M (1996) Phys Rev Lett 77:3865–3868
28. Pople JA, Head-Gordon M, Raghavachari K (1987) J Chem Phys 87:5968–5975
29. Scuseria GE, Schaefer HF III (1989) J Chem Phys 90:3700–3703
30. Scuseria GE, Janssen CL, Schaefer HF III (1988) J Chem Phys 89:7382–7387
31. Stuttgart RSC (1997) ECP basis sets used in this work and the related references therein can be obtained from https://bse.pnl.gov/bse/portal
32. Frisch MJ, Trucks GM, Schlegel HB, Scuseria GE, Robb MA, Cheeseman JR, Montgomery JA, Vreven T, Kudin KN, Burant JC, Millam JM, Iyengar SS, Tomasi J, Barone V, Mennucci B, Cossi M, Scalmani G, Rega N, Petersson GA, Nakatsuji H, Kitao O, Nakai H, Klene M, Li X, Knox JE, Hratchian HP, Cross JB, Adamo C, Jaramillo J, Gomperts R, Stratmann RE, Yazyev O, Austin AJ, Cammi R, Pomelli C, Ochterski JW, Ayala PY, Morokuma K, Voth GA, Salvador P, Dannenberg JJ, Zakrzewski VG, Dapprich S, Daniels AD, Strain MC, Farkas O, Malick DK, Rabuck AD, Raghavachari K, Foresman JB, Ortiz JV, Cui Q, Baboul AG, Clifford S, Cioslowski J, Stefanov BB, Liu A, Liashenko A, Piskorz P, Komaromi I, Martin RL, Fox DJ, Keith

T, Al-Laham MA, Peng CY, Nanayakkara A, Challacombe M, Gill PMW, Johnson BG, Chen W, Wang MW, Gonzales C, Pople JA (2003) Gaussian 03; Revision A.1. Gaussian Inc, Pittsburgh
33. Glendening ED, Badenhoop JK, Reed AE, Carpenter JE, Bohmann JA, Morales CM, Weinhold F (2001) NBO 5.0. Theoretical Chemistry Institute, University of Wisconsin, Madison
34. Singh NJ, Min SK, Kim DY, Kim KS (2009) J Chem Theory Comput 5:515–529
35. Dargel TK, Hertwig RH, Koch W (1999) Mol Phys 96:583–591
36. Siu FM, Ma NL, Tsang CW (2001) J Am Chem Soc 123:3397–3398
37. Zhu LY, Wang JL (2009) J Phys Chem C 113:8767–8771
38. Xiang HJ, Yang JL, Hou JG, Zhu QS (2006) J Am Chem Soc 128:2310–2314
39. Wang JL, Zhu LY, Zhang XY, Yang ML (2008) J Phys Chem A 11:8226–8230
40. Miyajima K, Nakajima A, Yabushita S, Knickelbein MB, Kaya K (2004) J Am Chem Soc 126:13202–13203